RSC Advances

ROYAL SOCIETY OF CHEMISTRY

www.rsc.org/advances

Dynamic Article Links ►

Cite this: DOI: 10.1039/c0xx00000x

www.rsc.org/xxxxxx

ARTICLE TYPE

Rhodium(0) nanoparticles supported on nanotitania as highly active catalyst in hydrogen generation from the hydrolysis of ammonia borane

Serdar Akbayrak,[a] Serap Gençtürk,[b] İzzet Morkan[b] and Saim Özkar*[a]

Received (in XXX, XXX) Xth XXXXXXXXX 20XX, Accepted Xth XXXXXXXXX 20XX

DOI: 10.1039/b000000x

Rhodium(0) nanoparticles supported on the surface of titanium dioxide (Rh(0)@TiO$_2$) were in situ generated from the reduction of rhodium(III) ions impregnated on nanotitania during the hydrolysis of ammonia borane. They were isolated from the reaction solution by centrifugation and characterized by a combination of advanced analytical techniques. The results show that (i) highly dispersed rhodium(0) nanoparticles of size in the range 1.3-3.8 nm were formed on the surface of titanium dioxide, (ii) Rh(0)@TiO$_2$ show high catalytic activity in hydrogen generation from the hydrolysis of ammonia borane with a turnover frequency value up to 260 min-1 at 25.0 ± 0.1 ºC, (iii) the results of kinetic study on the hydrogen generation from the hydrolysis of ammonia borane were also reported including the activation energy of 65.5 ± 2 kJ/mol for this reaction.

Introduction

Ammonia-borane (NH_3BH_3, AB) has been regarded as one of the leading candidates as hydrogen storage materials for on-board hydrogen applications due to its high hydrogen storage capacity (19.6 wt %), nontoxicity and high stability under ambient conditions.[1] Hydrogen stored in the AB complex can be released by either thermolysis [2] or solvolysis.[3] Since the high temperature is required for the former,[4] the latter reaction is highly advantageous for the hydrogen generation from AB. However, hydrogen stored in AB can be released at appreciable rate via hydrolysis only in the presence of a suitable catalyst (eq.1).[5,6] Therefore, the development of efficient and stable catalysts under moderate conditions is vital for the practical applications.

$$H_3NBH_3(aq)+2H_2O(l) \xrightarrow{catalyst} NH_4^+(aq) + BO_2^-(aq) + 3\,H_2(g) \qquad (1)$$

A number of catalysts have been tested in hydrogen generation from the hydrolysis of AB, including transition metal nanoparticles such as platinum, rhodium, ruthenium, palladium, cobalt and nickel.[7,8] Although rhodium, platinum and ruthenium metal nanoparticles have high price and limited abundance, they are superior to the non-noble metal nanoparticles due to their long life-time and high activity in the hydrolysis of ammonia borane. Therefore the use of noble metal nanoparticles as catalysts has been intensively studied in recent years. Metal nanoparticles exhibit much higher catalytic activity compared to the bulk metal due to the large fraction of atoms on their surface. However, metal nanoparticles tend to aggregate into clumps causing a decrease in catalytic activity.[9,10] Titanium dioxide with large surface area ranging from 10 to 300 m^2/g can be used as a support to prevent the aggregation of metal nanoparticles. Titanium dioxide is one of the suitable catalysts for environmental applications because of its nontoxicity, strong oxidizing power and the high stability against corrosion.[11] Titanium dioxide has also been extensively studied as a semiconductor material due to its wide band gap and low cost.[12]

Herein we report the *in situ* generation, characterization, and catalytic use of rhodium(0) nanoparticles supported on titanium dioxide with particle size of about 100 nm, hereafter referred to as Rh(0)@TiO$_2$. Rhodium(III) ions impregnated on the surface of titania particles was reduced by ammonia borane forming the Rh(0)@TiO$_2$ without using any additional reducing agent during the hydrolysis of ammonia borane. The use of *in situ* generation of Rh(0)@TiO$_2$ provides the opportunity to avoid the laborious catalyst preparation steps. Rh(0)@TiO$_2$ were isolated from the reaction solution and characterized by ICP-OES, XRD, TEM, SEM-EDS, XPS and the N$_2$ adsorption–desorption techniques. Our report also includes the following major findings: (*i*) Formation of highly dispersed rhodium(0) nanoparticles on the surface of titanium dioxide with particle size in the range 1.3-3.8 nm. (*ii*) Remarkable catalytic activity of Rh(0)@TiO$_2$ in hydrogen generation from the hydrolysis of AB with a turnover frequency of 260 min^{-1} at 25 ± 0.1 °C. (*iii*) Reusability of Rh(0)@TiO$_2$ providing the complete hydrolysis of AB generating 3 mole H$_2$ per mole of AB even in the fifth use of the catalyst.

Experimental Section

Materials

Rhodium(III) chloride trihydrate ($RhCl_3{\cdot}3H_2O$), titanium(IV) oxide (anatase), and ammonia-borane (AB, 97%) were purchased from Aldrich. Deionized water was distilled by water purification system (Milli-Q System). All glassware and Teflon-coated magnetic stir bars were cleaned with acetone, followed by copious rinsing with distilled water before drying in an oven at 150 ºC.

Characterization

The rhodium content of the Rh(0)@TiO_2 sample was determined by Inductively Coupled Plasma Optical Emission Spectroscopy (ICP-OES, Leeman-Direct Reading Echelle) after the sample was completely dissolved in the mixture of HNO_3/HCl (1/3 ratio). Transmission electron microscopy (TEM) was performed on a JEM-2100F (JEOL) microscope operating at 200 kV. A small amount of powder sample was placed on the holey carbon grid of the transmission electron microscope. Samples were examined at magnification between 100 and 400 K. Scanning electron microscope (SEM) images were taken using a JEOL JSM-5310LV at 15 kV and 33 Pa in a high-vacuum mode without metal coating on carbon support. The X-ray photoelectron spectroscopy (XPS) analysis was performed on a Physical Electronics 5800 spectrometer equipped with a hemispherical analyzer and using monochromatic Al Kα radiation of 1486.6 eV, the X-ray tube working at 15 kV, 350W and pass energy of 23.5 keV. ^{11}B NMR spectra were recorded on a Bruker Avance DPX 400 with an operating frequency of 128.15 MHz for ^{11}B.

Preparation of rhodium(III) ions impregnated on TiO_2

TiO_2 (1000 mg) was added to a solution of $RhCl_3 \cdot 3H_2O$ (53.97 mg) in 100 mL H_2O in a beaker. This slurry was stirred at room temperature for 72 h and then Rh^{3+}@TiO_2 sample was isolated by centrifugation and washed with 100 mL of distilled water and the remnant was dried at 120 °C for 12 h in the oven.

In situ formation of rhodium(0) nanoparticles supported on TiO_2 and concomitant catalytic hydrolysis of AB

Rhodium(0) nanoparticles supported on TiO_2 (Rh(0)@TiO_2) were *in situ* generated from the reduction of Rh^{3+}@TiO_2 during the catalytic hydrolysis of AB. Before starting the catalyst formation and concomitant catalytic hydrolysis of AB, a jacketed reaction flask (20 mL) containing a Teflon-coated stir bar was placed on a magnetic stirrer (Heidolph MR-301) and thermostated to 25.0 ± 0.1 °C by circulating water through its jacket from a constant temperature bath. Then, a graduated glass tube (60 cm in height and 3.0 cm in diameter) filled with water was connected to the reaction flask to measure the volume of the hydrogen gas to be evolved from the reaction. Next, 20 mg powder of Rh^{3+}@TiO_2 (0.24 wt.% Rh) was dispersed in 10 mL distilled water in the reaction flask thermostated at 25.0 ± 0.1 °C. Then, 31.8 mg AB (1.0 mmol $H_3N.BH_3$) was added into the flask and the reaction medium was stirred at 1000 rpm. After adding ammonia borane, rhodium(0) nanoparticles were formed and the catalytic hydrolysis of AB started immediately. The volume of hydrogen gas evolved was measured by recording the displacement of water level every 30 s at constant atmospheric pressure of 693 Torr. The reaction was stopped when no more hydrogen evolution was observed. In each experiment, the resulting solutions were filtered and the filtrates were analyzed by ^{11}B NMR and conversion of AB to metaborate anion was confirmed by comparing the intensity of signals in the ^{11}B NMR spectra of the filtrates.

Determination of activation energy for hydrolysis of AB catalyzed by Rh(0)@TiO_2

In a typical experiment, the hydrolysis reaction was performed starting with 10 mL of 100 mM (31.8 mg) AB solution and 20 mg Rh^{3+}@TiO_2 (0.24 % wt. rhodium, [Rh] = 0.046 mM) at various temperatures (25, 30, 35, 40, 45 °C) in order to obtain the activation energy.

Reusability of Rh(0)@TiO_2 in hydrolysis of AB

After the complete hydrolysis of AB started with 10 mL of 100 mM AB (31.8 mg H_3NBH_3), and 100 mg Rh^{3+}@TiO_2 (0.24 % wt. Rhodium, [Rh] = 0.233 mM) at 25 ± 0.1 °C, the catalyst was isolated as a powder by centrifugation and dried at 120 °C in the oven after washing with 20 mL of water. The isolated samples of Rh(0)@TiO_2 were weighed and redispersed in 10 mL solution of 100 mM AB for a subsequent run of hydrolysis at 25 ± 0.1 °C.

Determination of the catalytic lifetime of Rh(0)@TiO_2 in the hydrolysis of AB

The catalytic lifetime of Rh(0)@TiO_2 in the hydrolysis of AB was determined by measuring the total turnover number (TTO). Such a lifetime experiment was started with a 50 mL solution containing 0.046 mM Rh(0)@TiO_2 and 30 mM AB at 25.0 ± 0.1 °C. When all the ammonia-borane present in the solution was completely hydrolyzed, more AB was added and the reaction was continued in this way until no hydrogen gas evolution was observed.

RESULTS AND DISCUSSION

Rhodium(0) nanoparticles supported on titanium dioxide were *in situ* generated from the reduction of Rh^{3+}@TiO_2 during the catalytic hydrolysis of AB. First, rhodium(III) ions were impregnated on titania with particle size of 100 nm from the aqueous solution of rhodium(III) chloride yielding Rh^{3+}@TiO_2 and then reduced by AB at room temperature. Both reduction of rhodium(III) to rhodium(0) and hydrogen release from the hydrolysis of AB occur concomitantly when AB solution is added to a suspension of Rh^{3+}@TiO_2. The progress of hydrolysis of AB was followed by monitoring the change in hydrogen pressure which was then converted into the equivalent H_2 per mole of AB, using the known 3:1 H_2/AB stoichiometry (eq 1).

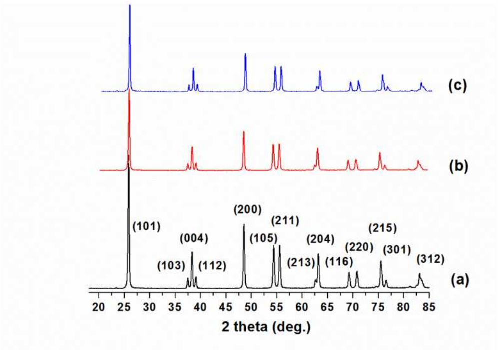

Figure 1: Powder XRD patterns of (a) TiO_2, (b) Rh^{3+}@TiO_2, (c) Rh(0)@ TiO_2 with a 0.24 % wt. Rh loading.

Characterization of rhodium(0) nanoparticles supported on TiO_2

Rhodium(0) nanoparticles supported on titania (Rh(0)@TiO_2), *in situ* formed during the hydrolysis of AB, could be isolated from the reaction solution as powder by centrifugation and characterized by ICP-OES, XRD, SEM-EDS, TEM, XPS and the N_2 adsorption-desorption techniques. Rhodium content of Rh(0)@TiO_2 was determined by ICP-OES and found as 0.24 % wt. Rh loading on titania surface. The N_2 adsorption-desorption analysis gave the surface area of titania as 10.71 m^2/g. Since the rhodium content of Rh(0)@TiO_2 was very low, it is difficult to understand the existence of rhodium(0) nanoparticles on the surface of titania by N_2 adsorption-desorption analysis. Comparison of the XRD patterns of TiO_2, Rh^{3+}@ TiO_2 and Rh(0)@TiO_2 with a rhodium loading of 0.24 wt.% Rh, given in Figures 1a, 1b, and 1c, respectively, clearly shows that there is no change in the characteristic diffraction peaks of TiO_2 (PDF Card 21-1272). This observation indicates that the host material remains intact after impregnation and reduction of rhodium(III) ions; there is no noticeable alteration in the framework lattice or change in the crystallinity. There is no observable peak attributable to rhodium nanoparticles in Figure 1b and 1c, probably because of low rhodium loading of TiO_2.

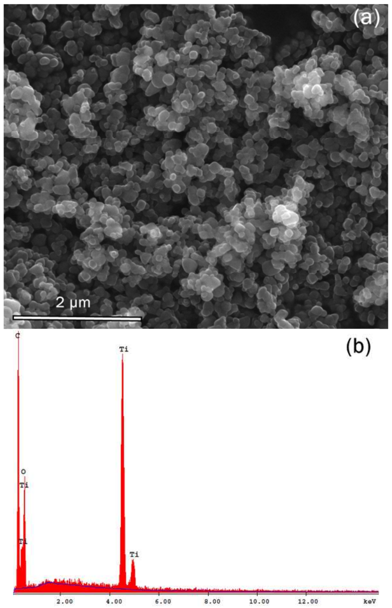

Figure 2: (a) SEM image and (b) SEM-EDS spectrum of Rh(0)@TiO_2 with a 0.24 % wt. Rh loading

SEM image of Rh(0)@TiO_2 with a rhodium loading of 0.24 % wt. in Figure 2a shows the presence of nearly monodispersed titania nanoparticles of 100 nm size. SEM-EDS spectrum of Rh(0)@TiO_2 with a rhodium loading of 0.24 % wt. in Figure 2b indicates the presence of the framework elements of TiO_2 (Ti, O). Since the low rhodium loading on TiO_2, the presence of rhodium nanoparticles could not be observed in SEM analysis.

Figure 3 shows the TEM images of Rh(0)@TiO_2 with a rhodium loading of 0.24 % wt. taken with different magnifications, which indicate that (*i*) highly dispersed rhodium(0) nanoparticles are formed on the surface of TiO_2 with particle size in the range 1.3-3.8 nm (mean diameter: 2.8 ± 0.7 nm) and (*ii*) the impregnation of rhodium(III) followed by reduction to rhodium(0) causes no change in the framework lattice of titania in agreement with the XRD results.

The composition of Rh(0)@TiO_2 formed *in situ* during the hydrolysis of AB and the oxidation state of rhodium were also studied by XPS technique. The survey-scan XPS spectrum of Rh(0)@TiO_2 with a rhodium loading of 0.24 % wt. (Fig. 4) shows that rhodium is the only element detected in addition to the TiO_2 framework elements (Ti, O). High resolution Rh 3d XPS of a Rh(0)@TiO_2 sample given in the inset of Figure 4 shows two prominent bands at 305.8 eV and 311.4 eV which can readily be assigned to rhodium(0) $3d_{5/2}$ and $3d_{3/2}$, resğpectively.[13,14] The bands at 309.7 eV and 313.8 eV (in green color in the inset of Figure 4), might be attributed to rhodium oxides, which might be formed during the XPS sampling.[14]

Catalytic Activity of Rh(0)@TiO_2 in hydrolysis of AB

Before starting with the investigation on the catalytic activity of Rh(0)@TiO_2 in the hydrolysis of AB, a control experiment was performed to check whether titanium dioxide shows any catalytic activity in the hydrolysis of AB at the same temperature used in

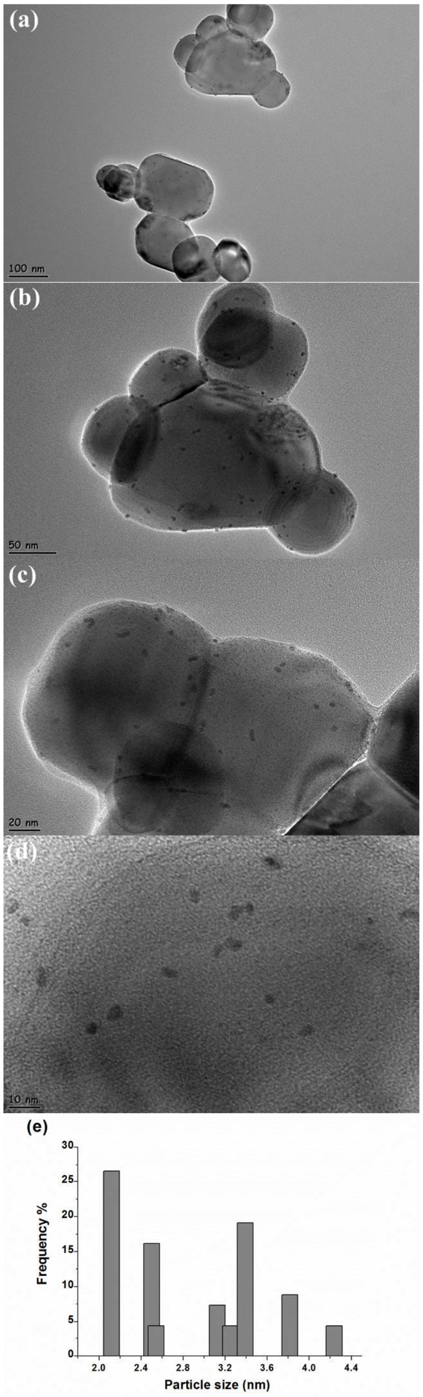

Figure 3: TEM image of Rh(0)@TiO_2 with a rhodium loading of 0.24 % wt. at (a) 100 nm, (b) 50 nm, (c) 20 nm, (d) 10 nm, (e) Histogram of Rh(0)@TiO_2 showing particle size distribution

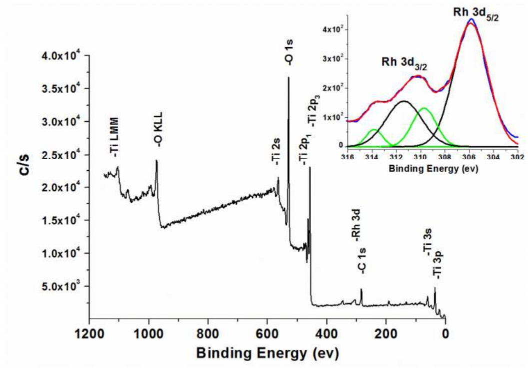

Figure 4: X-ray photoelectron (XPS) spectrum of Rh(0)@TiO_2 sample with a rhodium loading of 0.24 % wt. Rh. The inset gives the high resolution scan and deconvolution of Rh 3d bands.

this study. In a control experiment starting with 1.0 mmol of AB and 20 mg of powder of TiO_2 (the same amount as the one used in catalytic activity tests) in 10 mL of water at 25.0 ± 0.1 °C or 45.0 ± 0.1 °C, no hydrogen evolution was observed in 1 h at both temperatures. This observation indicates that the hydrolysis of AB does not occur in the presence of TiO_2 in the temperature range used in this study. However, Rh(0)@TiO_2 are found to be highly active catalyst in the hydrolysis of AB generating 3.0 equivalent H_2 gas per mole of AB in the same temperature range. Figure 5a shows the evolution of equivalent hydrogen per mole of AB versus time plot for the hydrolysis of AB (100 mM) using Rh(0)@TiO_2 as catalyst in different rhodium concentration at 25.0 ± 0.1 °C. The hydrogen generation rate was determined from the linear portion of each plot. For all tests a complete hydrogen release (mol H_2/mol H_3NBH_3 = 3) was observed. Figure 5b shows the plot of hydrogen generation rate versus initial concentration of rhodium, both in logarithmic scale, which gives a straight line with a slope of 1.12 indicating that hydrolysis of AB is first order with respect to the rhodium concentration. The turnover frequency (TOF), mol of H_2 per mol of rhodium per minute, for hydrogen generation from the hydrolysis of AB (100 mM) at 25.0 ± 0.1 °C was determined from the hydrogen generation rate in the linear portion of plots given in Figure 5a for experiments starting with 100 mM AB plus Rh(0)@TiO_2 with a loading of 0.24 % wt. Rh. The TOF value of Rh(0)@TiO_2 catalyst is as high as 260 min^{-1} (mol H_2/mol Rh.min) in hydrolysis of AB at 25.0 ± 0.1 °C. TOF values of the reported catalysts used in the hydrolysis of AB are listed in Table 1 for comparison. As clearly seen from the comparison of values listed in Table 1, Rh(0)@TiO_2 provide remarkable TOF value in the hydrolysis of AB as compared to the other ruthenium, rhodium and palladium catalysts.

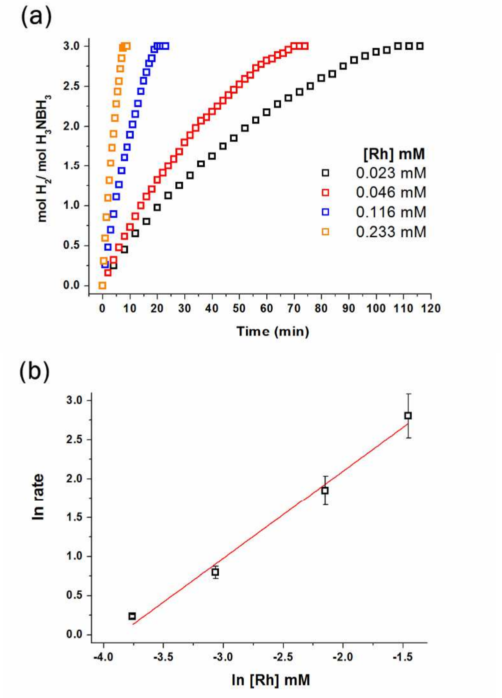

Figure 5: (a) mol H_2 /mol $H_3N.BH_3$ versus time graph depending on the rhodium concentration in Rh(0)@TiO_2 for the hydrolysis of AB (100 mM) at 25.0 ± 0.1 °C, (b) The logarithmic plot of hydrogen generation rate versus the concentration of Rh; *ln*(rate) = 1.12 *ln*[Rh] + 4.34.

The catalytic hydrolysis of AB was carried out at various temperature in the range of 25−45 °C starting with Rh(0)@TiO_2 (loading = 0.24 wt % Rh and [Rh] = 0.116 mM) plus 100 mM AB in 10 mL of water. The rate constants for the hydrogen generation at different temperatures were calculated from the slope of linear part of each plot given in Figure 6a and used for the calculation of activation energy (Ea = 65 ± 2 kJ/mol) from the Arrhenius plot in Figure 6b. The activation energy for hydrolysis of AB catalyzed by Rh(0)@TiO_2 is comparable to the literature values reported for the same reaction using other catalysts (see Table 1).

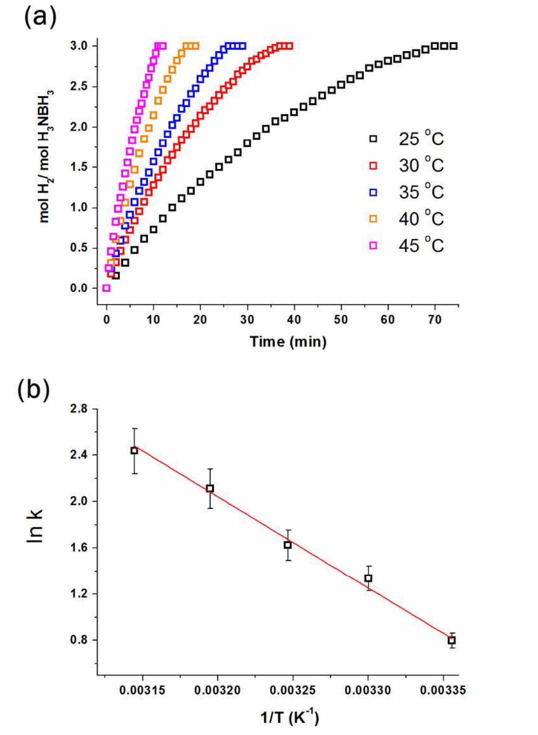

Figure 6: (a) The evolution of equivalent hydrogen per mole of AB versus time plot for the hydrolysis of AB starting with Rh(0)@TiO_2 (0.116 mM Rh) and 100 mM AB at various temperatures. (b) The Arrhenius plot for the Rh(0)@TiO_2 catalyzed hydrolysis of AB. *ln*k = -7883.5(1/T) +27.27.

Table 1: Catalytic activity of reported various catalysts used in the hydrolysis of AB

Entry	Catalyst	TOF (min^{-1})	Ea (kj/mol)	TTO	Ref
1	Ru@MWCNT	329	33	26,400	15
2	Rh(0)@TiO_2	260	65.5	37,350	This study
3	Laurate-stabilized Rh(0)	200	43.6	80,000	16
4	Ru(0)PSSA-co-MA	172	54	51,720	17
5	Ru(0)@Hap	137	58	87,000	18
6	Ni@Ru	114	44	-	19
7	Ru/Carbon	113	76	-	20
8	Ru/Graphene	100	11.7	-	21
9	ZFS Rh(0)	92	66.9	47,200	22
10	RuNPs@ZK-4	90.2	28	36,700	23
11	Ru(0)NP/Laurate	75	47	5,900	24
12	Pd@Co/graphene	37.5	-	-	25
13	$Co_{35}Pd_{65}$/C annealed	35.7	-	-	26
14	2.1 wt% RGO@Pd	26.3	40	-	27
15	Rh/γ-Al_2O_3	-	21	-	28

Reusability of Rh(0)@TiO_2 catalyst was tested in successive experiments performed using the catalyst isolated from the reaction solution after a previous run of hydrolysis of AB. After the completion of hydrogen generation from the hydrolysis of AB starting with 0.233 mM Rh^{3+}@TiO_2 plus 100 mM AB in 10 mL aqueous solution at 25.0 ± 0.1 °C, the catalyst was isolated by centrifugation and washed with 10 mL of water. After washing, the isolated sample of Rh(0)@TiO_2 was redispersed in 10 mL solution containing 100 mM AB and a second run of hydrolysis was started immediately and continued until the completion of hydrogen evolution. Hydrogen generation process was repeated five times. After the fifth use in hydrolysis of AB, Rh(0)@TiO_2 preserve only 7.0% of their initial catalytic activity. The reusability tests reveal that Rh(0)@TiO_2 are still active in the subsequent runs of hydrolysis of AB providing a release of 3.0 equivalent H_2 per mole of NH_3BH_3.

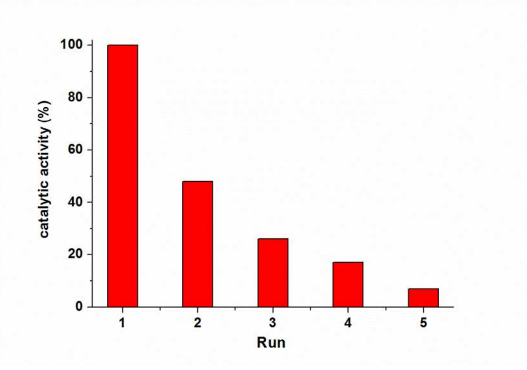

Figure 7: Percentage of initial catalytic activity of Rh(0)@TiO_2 ([Ru] = 0.233 mM) in successive runs after the reuse for the hydrolysis of ammonia borane (100 mM).

The catalytic activity of the filtrate solution obtained by centrifugation of the solid materials after the first run of hydrolysis was also tested in the hydrolysis of AB (100 mM) under the same conditions. As shown in Fig. 8, the filtrate solution shows no catalytic activity in the hydrolysis of AB. This observation supports the conclusion that there is no leaching of rhodium into the solution during the hydrolysis and suggests that the rhodium(0) nanoparticles supported on TiO_2 are kinetically competent and heterogeneous catalyst in the hydrolysis of ammonia borane.

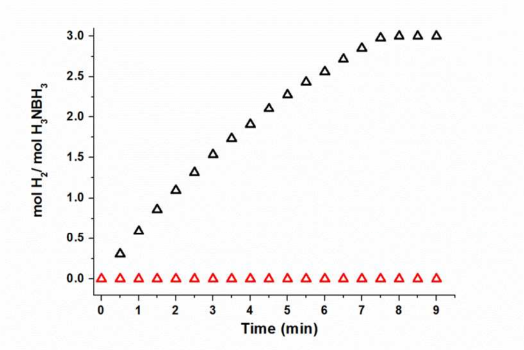

Figure 8: The evolution of equivalent hydrogen per mole of AB versus time plot for the hydrolysis of AB (100 mM) starting with Rh(0)@TiO_2 (0.233 mM Rh) (Δ), the filtrate solution obtained by centrifugation of the solid materials after the first run, (Δ), at room temperature.

Catalytic lifetime of Rh(0)@TiO_2 was determined by measuring the total turnover number (TTO) in the hydrolysis of ammonia borane. A catalyst lifetime experiment was performed starting with 20 mg Rh^{3+}@TiO_2 (rhodium loading = 0.24 % wt. Rh, and [Rh] = 0.0466 mM) in 100 mL solution of AB at 25.0 ± 0.1 °C. Figure 9 shows the variation in turnover number (TON) and turnover frequency (TOF) in the course of reaction. The TOF value decreases expectedly as the rhodium(0) nanoparticles catalysts are deactivated during the lifetime experiment because of the increasing concentration of metaborate ion. Rhodium(0) nanoparticles supported on TiO_2 provide 37,350 turnovers over 20 h in the hydrolysis of AB at 25.0 ± 0.1 °C before deactivation. As shown in Table 1, TTO value of Rh(0)@TiO_2 for the hydrolysis of ammonia borane is comparable to the literature values reported for the same reaction using other catalysts.

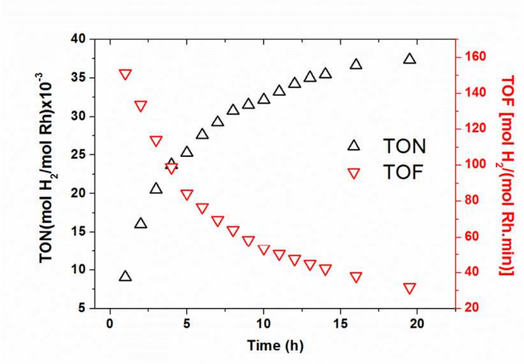

Figure 9: The variation in turnover number (TON) and turnover frequency (TOF) during the catalytic lifetime experiment performed starting with 20 mg Rh(0)@TiO_2 (rhodium loading = 0.24 % wt. Rh, and [Rh] = 0.0466 mM) in 100 mL solution of AB at 25.0 ± 0.1 °C.

Conclusions

In summary, rhodium(0) nanoparticles supported on titania were reproducibly prepared from the reduction of Rh^{3+}@TiO_2 during the catalytic hydrolysis of ammonia borane. Rhodium(III) ions were impregnated on titanium dioxide from the aqueous solution of rhodium(III) chloride and then reduced by ammonia borane at room temperature. Highly dispersed rhodium(0) nanoparticles with particle size in the range 1.3-3.8 nm on titanium dioxide were prepared and characterized by a combination of advanced analytical techniques. Rh(0)@ TiO_2 show high catalytic activity in hydrogen generation from the hydrolysis of ammonia borane providing a turnover frequency value up to 260 min^{-1} at 25.0 ± 0.1 ºC. Rh(0)@TiO_2 are long-lived catalyst providing 37,350 turnovers in hydrogen generation from the hydrolysis of ammonia borane at 25.0 ± 0.1 ºC. Rh(0)@TiO_2 are reusable catalyst as they provide the complete hydrolysis of ammonia borane generating 3 mole H_2 per mole of AB even in the fifth use. The results of quantitative kinetic study on the hydrogen generation from the hydrolysis of ammonia borane show that the hydrolysis reaction is first order in rhodium concentration and the activation energy is 65.5 ± 2 kJ/mol for the hydrogen generation catalyzed by Rh(0)@ TiO_2. High catalytic activity and simple preparation procedures make Rh(0)@TiO_2 very attractive catalysts for the hydrolysis of ammonia borane.

Acknowledgment

Partial support by Turkish Academy of Sciences is gratefully acknowledged. We would like to thank Seçkin Öztürk and İlker Yıldız for TEM and XPS analyses, respectively.

Notes and references

[a] *Department of Chemistry, Middle East Technical University,06800 Ankara, Turkey.Fax: +90 312 210 3200; Tel: +90 312 210 3212; E-mail: sozkar@metu.edu.tr*

[b] *Department of Chemistry, Abant İzzet Baysal University,14280 Bolu, Turkey Fax: +90 374 253 46 42; Tel: +90 374 254 1000-1246; E-mail: morkan_i@ibu.edu.tr*

1 T. Umegaki, J-M. Yan, X-B. Zhang, H. Shioyama, N. Kuriyama, Q. Xu, *Int. J. Hydrogen Energy*, 2009, **34**, 2303-2311.
2 M. Ramzan, F. Silvearv, A. Blomqvist, R.H. Scheicher, S. Lebeque, R. Ahuja, *Phys. Rev. B*, 2009, **79**, 132102-4.
3 Q. Xu, M. Chandra, *J. Power Sources*, 2006, **163**, 364-370.
4 G. Wolf, J. Baumann, J. Baitalow, F.P. Hoffmann, *Thermochim. Acta*, 343, **2000**, 19-25.
5 M.Yadav, Q. Xu, *Energy Environ. Sci.*, 2012, **5**, 9698-9725.
6 M. Zahmakıran, S. Özkar, *Nanoscale,* 2011, **3**, 3462-3481.
7 S. Özkar, S.L. Suib (Eds.), Batteries, Hydrogen Storage and Fuel Cells, Elsevier, Amsterdam, 2013.
8 Z.H. Lu, Q. Xu, *Func. Mater. Lett.*, 2012, **5**, 1230001-9.
9 S. Özkar, R.G. Finke, *J. Am. Chem. Soc.*, 2002, **124**, 5796-5810.
10 S. Özkar, R.G. Finke*, Langmuir*, 2002, **18**, 7653-7662.
11 O. K. Varghese, M. T. J. LaTempa, C. A. Grimes, *Nano Lett*., 2009, **9**, 731-737.
12 X. Chen, S. S. Mao, *Chem. Rev.*, 2007, **107**, 2891-2959.
13 Y. Baer, P.F. Heden, J. Hedman, M. Klasson, C. Nordling, K. Siegbahn, *Phys. Scripta*, 1970, **1**, 55-65.
14 V. Mevellec, A. Nowicki, A. Roucoux, C. Dujardin, P. Granger, E. Payen, K. Philippot, *New J. Chem.*, 2006, **30**, 1214-1219.
15 S. Akbayrak, S. Özkar, *ACS Appl. Mater. Interfaces*, 2012, **4**, 6302-6310.
16 F. Durap, M. Zahmakıran, S. Özkar, *Appl. Catal. A: General*, 2009, **369**, 53-59.
17 Ö. Metin, S. Sahin, S. Özkar, *Int. J. Hydrogen Energy*, 2009, **34**, 6304-6313.
18 S. Akbayrak, P. Erdek, S. Özkar, *Appl. Catal. B: Environ*., 2013, **142-143**, 187-195.
19 GZ. Chen, S. Desinan, R. Nechache, R. Rose, F. Rose, DL. Ma, *Chem. Commun*., 2011, **47,** 6308-6310.
20 S. Basu, A. Brockman, P. Gagare, Y. Zheng, P.V. Ramachandran, W.N. Delgass, J.P.Gore, *J. Power Sources*, 2009, **188**, 238-243.
21 N. Cao, W. Luo, G. Cheng, *Int. J. Hydrogen Energy*, 2013, **38**, 11964-72.
22 M. Zahmakıran, S. Özkar, *Appl. Catal. B: Environ*., 2009, **89**, 104-110.
23 M. Zahmakıran, *Mater. Sci. Eng. B*, 2012, **177**, 606-613.
24 F. Durap, M. Zahmakıran, S. Özkar, *Int. J. Hydrogen Energy*, 2009, **34**, 7223-7230.
25 J.Wang, Y-L. Qin, X. Liu, X-B. Zhang, *J. Mater. Chem*., 2012, **22**, 12468-12470.
26 D. Sun, V. Mazumder, Ö. Metin, S.Sun, *ACS Nano*, 2011, **5**, 6458-6464.
27 B. Kılıç, S. Şencanlı, Ö. Metin, *J. Molecular Catal. A: Chemical*, 2012, **361-362**, 104-110.
28 M. Chandra, Q. Xu, *J. Power Sources*, 2007, **168**, 135-142.

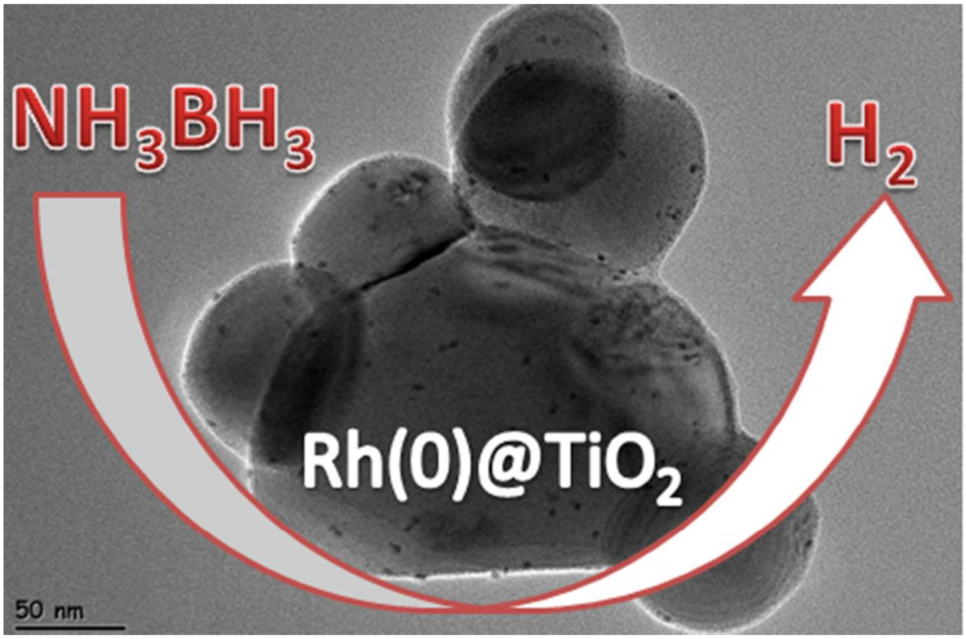

Rhodium(0) nanoparticles supported on nanotitania as highly active catalyst in hydrogen generation from the hydrolysis of ammonia borane
127x83mm (96 x 96 DPI)